J Mater Sci: Mater Med (2011) 22:853–863
DOI 10.1007/s10856-011-4262-2

Glycyrrhetinic acid-functionalized degradable micelles as liver-targeted drug carrier

Wei Huang · Wei Wang · Ping Wang · Chuang-Nian Zhang · Qin Tian · Yue Zhang · Xiu-Hua Wang · Rui-Tao Cha · Chun-Hong Wang · Zhi Yuan

Received: 23 April 2010 / Accepted: 17 February 2011 / Published online: 4 March 2011

Abstract Recently, many efforts have been devoted to investigating the application of functionalized micelles as targeted drug delivery carriers. In this study, glycyrrhetinic acid (GA, a liver targeting ligand) modified poly(ethylene glycol)-*b*-poly(γ-benzyl L-glutamate) micelles were prepared and evaluated as a potential liver-targeted drug carrier. The aggregation behavior, stability, size and morphology of the micelles were investigated. Anticancer drug doxorubicin (DOX) was encapsulated in the micelles. The drug release profile, in vivo distribution and the cytotoxicity against hepatic carcinoma QGY-7703 cells of DOX-loaded micelles were studied. The results indicated that the release profile was pH-dependent with Fickian diffusion kinetics. The micelles were remarkably targeted to the liver, inducing a 4.9-fold higher DOX concentration than that for free DOX·HCl. The DOX-loaded micelles exhibited almost twofold more potent cytotoxicity compared with DOX·HCl, and the cytotoxicity was time- and dosage-dependent. These results suggest that GA-functionalized micelles represent a promising carrier for drug delivery to the liver.

1 Introduction

Cancer is a major cause of mortality worldwide and its incidence is increasing annually. At present, cancer treatment mainly involves chemotherapy. However, chemotherapeutic drugs, such as doxorubicin (DOX), camptothecin and paclitaxel, cause serious systemic toxicity, induce multidrug resistance, and suffer from rapid phagocytic and renal clearance, which limit their clinic application [1, 2]. Therefore, the design and construction of ideal drug delivery systems has been an intense field of research [3–6]. An ideal drug carrier should meet several basic requirements, including high drug loading capacity, biodegradability, excellent stability in physiological environment, favorable biodistribution and controllable drug release profiles [7, 8].

Among various drug carriers, interest in polymeric micelles as promising drug delivery carriers has increased. These nano-sized micelles, especially formed from the self-assembly of amphiphilic block copolymer, possess a unique core–shell architecture in aqueous solution. The hydrophobic core serves as a nano-reservoir for therapeutic agents while the hydrophilic shell maintains a hydration barrier that can effectively stabilize the micelles in blood and reduce the uptake by the reticuloendothelial system (RES) [9–12]. Moreover, when the hydrophilic shell is decorated with ligand capable of binding specifically to the targeted site, the micelles can effectively ferry drugs to specific tissues or organs [13, 14]. This yields a sufficient drug concentration within the target cells via receptor-mediated endocytosis [15]. For example, Sung et al. prepared the galactosamine-conjugated poly(γ-glutamic acid)-*b*-poly(lactide) nanoparticles that mainly accumulated in rat liver via ligand-receptor recognition. In addition, a significant delay in hepatoma tumor growth was observed, indicating a potential application for targeted drug delivery to liver cancers [16].

Glycyrrhizin (GL) and glycyrrhetinic acid (GA, a hydrolysis product of GL) are the main components of liquorice and have been widely used in the prescription of traditional Chinese medicine [17, 18]. In 1991, Negishi reported that there are specific binding sites for GL and GA

W. Huang · W. Wang · P. Wang · C.-N. Zhang · Q. Tian · Y. Zhang · X.-H. Wang · R.-T. Cha · C.-H. Wang · Z. Yuan (✉)
Key Laboratory of Functional Polymer Materials, Ministry of Education, Institute of Polymer Chemistry, Nankai University, Tianjin 300071, China
e-mail: zhiy@nankai.edu.cn

on the cellular membrane of hepatocytes, and the number of binding sites for GA is much more than that for GL [19]. Later, Ismair et al. [20] confirmed that the uptake process of GL into hepatocytes was a carrier-mediated pathway. Therefore, a growing interest has been focused on the application of GA/GL as liver targeting ligands [21–27]. Tian et al. successfully prepared GA-modified chitosan/poly(ethylene glycol) nanoparticles (CTS/GA–PEG NPs), which were remarkably targeted to rat liver and exhibited a 2.6-fold higher accumulation in liver than that of the non-targeted group (CTS/PEG NPs) [24]. Lin et al. also found that the GL-modified nanoparticles were preferentially accumulated in hepatocytes via a ligand-receptor interaction [25]. Based on the above results, it could be concluded that GA/GL are effective ligands for liver targeting, which could enhance the accumulation of drug delivery system in the liver and further precisely deliver adequate amounts of drug to the liver cells.

In previous work conducted in our laboratory, liver-specific targeting polypeptides were fabricated from poly(γ-benzyl L-glutamate) (PBLG) with a liver targeting ligand GA at the distal end [27]. In the present study, hydrophilic poly(ethylene glycol) (PEG) was introduced between the GA and PBLG segments. This conferred the resultant GA–PEG–PBLG copolymer with amphiphilic character and facilitated micelles self-assembly in aqueous solution. The in vitro degradation profile and aggregation behavior of the copolymer were studied. Doxorubicin was encapsulated in the micelles by diafiltration. The in vitro release profile, the in vivo distribution behavior and the cytotoxicity against hepatic carcinoma QGY-7703 cells were investigated.

2 Materials and methods

2.1 Materials

Glycyrrhetininc acid (GA) was purchased from Fujie Pharmaceutical Limited Company (Xi'an, China). γ-benzyl glutamate (BLG) was supplied by Sichuan Tongsheng Amino acid Co. (Sichuan, China). Poly(ethylene glycol)-bis-amine (ATPEG, $M_n = 3350$), pyrene, dicyclohexylcarbodiimide (DCC), *N*-hydroxysuccinimide (NHS), DOX hydrochloride (DOX·HCl), RPMI-1640 medium, fetal bovine serum (FBS), 3-(4,5-dimethylthiazol-2-yl)-2,5-diphenyl tetrazolium bromide (MTT) were all purchased from Sigma-Aldrich (St. Louis, MO). Tetrahydrofuran (THF) was dried by distillation over potassium-sodium alloy. Dichloromethane (CH_2Cl_2) was dried by distillation with calcium hydride. All other regents were used as received without further purification. Hepatic carcinoma QGY-7703 cells and Wistar rats (200 ± 20 g) were brought from Tianjin Medical University.

2.2 Synthesis of GA–PEG–PBLG block copolymer

The γ-benzyl L-glutamate *N*-carboxyanhydride (BLG–NCA) monomer was synthesized according to the method of Daly [28].

The macro-initiator of GA-PEG-NH_2 was prepared in the similar procedure as reported by Steenis [29]. In brief, poly(ethylene glycol)-bis-amine (ATPEG) was reacted with GA at a molar ratio of 1:5 using DCC and NHS as condensing agents. The resultant GA-PEG-NH_2 was further used to initiate the ring-opening polymerization (ROP) of BLG–NCA according to the method described by Ponchel's group [30]. The reaction mixture was stirred at room temperature (r.t.) until the characteristic NCA bands disappeared from the Fourier transform infrared assay (FTIR, Bio-Rad 135). The whole synthetic route is illustrated in Scheme 1.

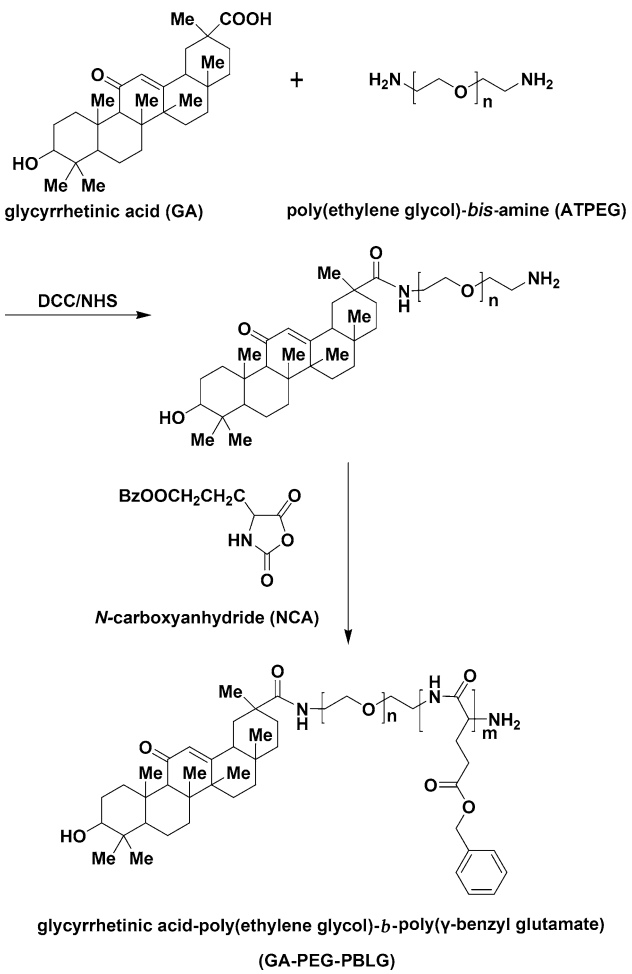

Scheme 1 Synthetic route for GA–PEG–PBLG copolymer

2.3 Characterization of the copolymer

The structure of the GA–PEG–PBLG copolymer was determined on a Varian Unity-Plus 400 NMR spectrometer, using tetramethylsilane as the internal standard and $CDCl_3$ as the solvent. The structure was also confirmed by FTIR measurement at r.t. on the polymer powders. Molecular weight and polydispersity index (PDI) of GA–PEG–PBLG copolymer were determined in THF by gel permeation chromatography (GPC). (Apparatus: Water 515 pump, Waters 2410 refractive index detector, flow rate: 1 ml/min, polystyrene standards).

2.4 Polymer degradation

The degradation behavior of the GA–PEG–PBLG copolymer was evaluated in phosphate buffer solution (PBS, pH 7.4, 5.8) according to the literature with minor modification [31]. Briefly, the copolymer (120 mg) was dissolved in 2 ml of dichloromethane (CH_2Cl_2) in a 15-mm internal diameter glass vial. After the solvent was evaporated, 10 ml of PBS was added, and the vial was then placed in an incubator at 37°C at a speed of 100 rpm. At predetermined time intervals, samples were washed with distilled water, dried and weighed. The weight loss of the sample was calculated by Eq. 1:

$$\text{Weight loss } (\%) = (W_0 - W_t)/W_0 \times 100\% \quad (1)$$

where W_0 is the initial weight of the copolymer, and W_t is the weight of the copolymer at time t.

2.5 Determination of critical micelle concentration

The critical micelle concentration (CMC) of the amphiphilic copolymer in aqueous solution was determined by spectrofluorometer (F-7000, Hitachi, Japan). Pyrene was chosen as a hydrophobic fluorescent probe. Aliquots of pyrene solutions in acetone (6.5×10^{-7} mol/l, 20 μl) were added to each vial, and then acetone was allowed to evaporate. Copolymer suspensions (10 ml) with different concentrations were added to each vial and kept at r.t. for 24 h to equilibrate the pyrene in the aqueous phase. Excitation wavelength was 336 nm, and the emission spectra were recorded from 360 to 440 nm. The slit openings for excitation and emission were set at 10 and 2.5 nm, respectively.

2.6 Preparation and characterization of micelles

Doxorubicin-loaded micelles were prepared by diafiltration as reported previously [32]. In brief, 20 mg of block copolymer was dissolved in 4 ml of *N,N′*-dimethylformamide (DMF), and then DOX·HCl in 1 ml of DMF was added with various feed weight ratio to copolymer (DOX/copolymer = 0.05–0.20). Triethylamine (TEA) was added to the mixture for dehydrochlorination of DOX·HCl. The mixture was dialyzed against acetate buffer (0.1 M, pH 5.5) for 2 h and then against distilled water to remove free drug and organic solvents (molecular cut-off: 7×10^3 Da). The resultant suspension was lyophilized. Blank polymeric micelles were fabricated in the same way without the addition of DOX.

The hydrodynamic diameter of the micelles was determined by dynamic laser scattering (90 Plus Particle Size Analyzer, Brookhaven Instruments Co.). The scattering angle was kept at 90°. The wavelength was set as 633 nm and the standard was water during the whole experiment. Data were analyzed by a CONTIN analytic method. The morphology of the micelles was characterized by atomic force microscopy (AFM, Mutimode Scanning Probe Microscope, Digital Instruments) with Nanoscope IIIa by applying the tapping mode. The AFM sample was prepared by placing a drop of the micelle suspension on a mica slide and then dried in vacuum. Data were analyzed by V5.30r3sr3 software.

2.7 Stability evaluation of micelles in BSA

A basic evaluation of the stability for GA–PEG–PBLG micelles was conducted in PBS containing 1 wt% bovine serum albumin (BSA) at 37°C [33]. At predetermined time intervals, the turbidity changes of the micelle solution were monitored via UV–Vis spectroscopy at 390 nm.

2.8 Drug encapsulation

To determine the drug content in the micelles, weight amount of DOX-loaded micelles were dissolved in DMF. The DOX concentration was determined from UV absorbance at 485 nm with reference to a calibration curve of DOX in DMF. The drug loading content (DLC) and drug loading efficiency (DLE) were calculated based on Eqs. 2 and 3, respectively.

$$\text{DLC } (\%) = (\text{weight of loaded DOX/weight of micelles}) \times 100\% \quad (2)$$

$$\text{DLE } (\%) = (\text{weight of loaded DOX/weight of drug in feed}) \times 100\%. \quad (3)$$

2.9 In vitro release study and the release mechanism

The in vitro release profiles of DOX from micelles were performed in PBS of pH 5.8 and 7.4, respectively. The freeze-dried micelles were weighed and re-suspended in PBS at a concentration of 1 mg/ml, the suspension was then transferred to a centrifuge tube and shaken at a speed

of 100 rpm. At scheduled time intervals, supernatants were isolated by centrifugation and replaced with fresh PBS. The DOX content in the supernatants was measured by Waters 484 HPLC (USA) equipped with a reverse-phase C_{18} column (250 × 4.6 mm) at a flow rate of 1 mL/min. The mobile phase was a mixture of CH_3OH:CH_3CN:H_2O:H_3PO_4 = 12:100:112:0.15 (v/v). The cumulative amount of DOX released from micelles was plotted against time.

In addition, the drug release mechanism was investigated by applying the following mathematical model (Eq. 4):

$$\log(M_t/M_\infty) = \log k + n\log t. \quad (4)$$

where M_t/M_∞ denotes the fractional amount of the drug released at time t. k is a kinetic constant that measures the drug release rate, and n is a diffusion exponent which is indicative of the release mechanism. From the slope and intercept of the plot of $\log(M_t/M_\infty)$ versus $\log t$, kinetic parameters k and n are calculated [34].

2.10 In vivo biodistribution study

The in vivo DOX biodistribution in rats was investigated according to the literature with minor modification [35]. All of the procedures involved in the animal experiments were performed in strict accordance with institutional guidelines (Institutional Animal Care and Use Committee Approval. No. SCXK-2007-004). In brief, Wistar rats (five rats per group) received a single intravenous injection of DOX·HCl or DOX/GA–PEG–PBLG micelle solution at a DOX equivalent dose of 5 mg/kg in PBS. At 2 h post-treatment, tissues samples were harvested, weighed and homogenized with PBS. The resultant tissue homogenates were suspended in HCl/ethanol mixture, followed by vigorous vortex-mixing. After a further step of centrifugation, DOX fluorescence in the supernatant was measured with a spectrofluorometer (F-7000, Hitachi, Japan) using a pre-established standard curve.

2.11 Cytotoxicity assay

Methyl thiazolyl tetrazolium (MTT) assay was adopted to compare the cytotoxicity of DOX·HCl and DOX/GA–PEG–PBLG micelles against hepatic carcinoma QGY-7703 cells. Cells in the log phase were seeded in 96-well plates at a density of 5×10^3 cells per well, followed by incubating in media containing different DOX formulations. The amount of DOX/GA–PEG–PBLG micelles was calculated based on the DLC value. At predetermined time, the media were discarded and MTT solution (5 mg/ml) was added for additional 4 h. Subsequently, 200 μl of dimethyl sulfoxide (DMSO) was added to each well to ensure the solubilization of formazan crystal. The optical density (OD) was measured at 570 nm with a Microplate Reader Model 550 (Bio-Rad, USA). The cytotoxicity was calculated by Eq. 5:

$$\text{Cytotoxicity} = (A - B)/A \times 100\% \quad (5)$$

where A is the absorbance of the cells treated with culture medium, and B is the absorbance of the cells incubated with DOX·HCl or DOX/GA–PEG–PBLG micelles.

2.12 Statistical analysis

All data expressed as means ± SD deviation (S.D.) are representative of at least three different experiments. Statistical analysis was performed in Origin 7.0. A two-tailed paired Student's t test was used to compare the differences. A value of $P < 0.05$ was considered statistically significant.

3 Results

3.1 Synthesis and characterization of GA–PEG–PBLG copolymer

In this paper, PBLG derivatives were synthesized by ROP of BLG–NCA using GA–PEG–NH_2 as the initiator (Scheme 1). Polymerization process was monitored via FTIR spectroscopy. Disappearance of absorption bands at 1860 and 1781 cm^{-1} corresponding to the C=O of the anhydride, indicating the completion of the ROP. Moreover, the amide I band, amide II band and amide III band in the spectrum of GA–PEG–PBLG copolymer are located at 1651, 1545 and 1255 cm^{-1} respectively, suggesting a typical α-helical conformation is detected for the PBLG segment. Such results are also found in Ponchel's research with PBLG derivatives [30].

The structure of the GA–PEG–PBLG copolymer was also verified by ^{1}H-NMR measurement. The chemical shifts are assigned as follows: δ = 7.08–7.35 ppm (75 H, H_{arom}), 4.95–5.05 ppm (30 H, H_{benzyl}), 3.82–3.99 ppm (15 H, $H_{\alpha\text{-Glu}}$), 2.46–2.60 ppm (30 H, $H_{\gamma\text{-Glu}}$), 2.14–2.32 ppm (30 H, $H_{\beta\text{-Glu}}$), 3.52–3.68 ppm (304 H, CH_2CH_2O), 0.64–1.37 ppm (43 H, typical protons of GA moiety). As the molecular weight of PEG segment is known, we can easily calculate the PDI of PBLG and the number-average molecular weight (M_n) of the copolymer based on the relative peak intensities of methane protons (δ = 3.65 ppm) of PEG and methane protons (δ = 5.05 ppm) of PBLG. The polymerization degree is 14.9, and the M_n of the copolymer is 7.06×10^3 Da. Besides, the M_n of the copolymer determined by GPC is 6.88×10^3 Da, and the PDI is relatively narrow (PDI = 1.09).

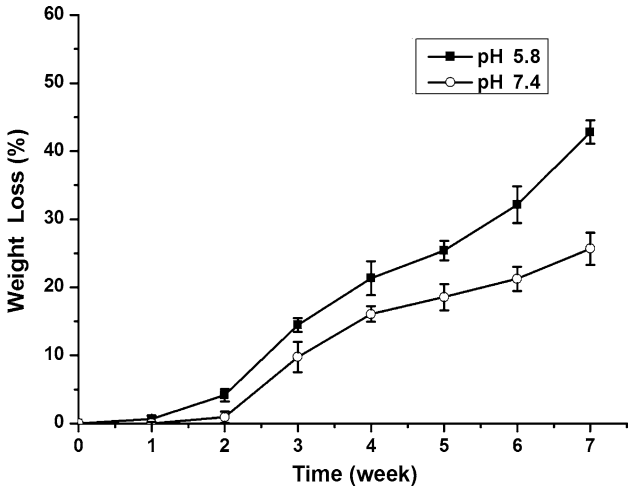

Fig. 1 Weight loss profiles of GA–PEG–PBLG copolymer in neutral (pH 7.4) and acidic (pH 5.8) media as a function of incubation time, mean ± SD ($n = 3$)

3.2 In vitro degradation behavior of GA–PEG–PBLG copolymer

The in vitro degradation behavior of GA–PEG–PBLG copolymer was investigated by measuring weight loss as a function of time. PBS of different pH was used to simulate the environment around cancer lesions (pH 5.8) and normal physiology (pH 7.4). The results are shown in Fig. 1. The copolymer weight under both pH conditions was almost constant during the first week. However, obvious weight loss could be observed after 2 weeks, indicating the degradation rate accelerated. The total weight loss for GA–PEG–PBLG copolymer under acidic and neutral conditions after 7 weeks was 42.8 and 25.6%, respectively.

3.3 Stability of GA–PEG–PBLG micelles

As shown in Fig. 2a, the fluorescent intensity increased with the increasing copolymer concentration, suggesting the formation of GA–PEG–PBLG aggregation and transfer of pyrene from the aqueous phase into the hydrophobic PBLG core. The fluorescence intensity ratio of the first (373 nm) and third (383 nm) highest energy bands (I_{373}/I_{383}) in pyrene excitation spectra was analyzed as a logarithm function of the copolymer concentration (log C). As shown in Fig. 2b, I_{373}/I_{383} was nearly constant at low copolymer concentration, and then decreased linearly as the copolymer concentration increased. The CMC calculated from the inflexion of this plot is 7.16 μg/ml.

The size and morphology of GA–PEG–PBLG micelles were analyzed by DLS (Fig. 3a) and AFM (Fig. 3b), respectively. Figure 3a indicated that the micelles had a narrow size distribution with an average hydrodynamic diameter of approximately 181 nm. Figure 3b showed that the micelles were spherical in shape with a smooth surface, and formed discrete particles with a diameter about 160 nm. Notably, the particle size determined by AFM was slightly smaller than the DLS result. This difference is mainly due to micelle shrinkage and collapse during the drying process for AFM measurement.

The stability of GA–PEG–PBLG micelles was also evaluated by measuring the turbidity changes in the presence of BSA. As shown in Fig. 4, minimal turbidity changes were detected, indicating that the micelles were highly stable. This result is in good agreement with Ponchel's researches conducted on PEGylated particles [30, 36, 37].

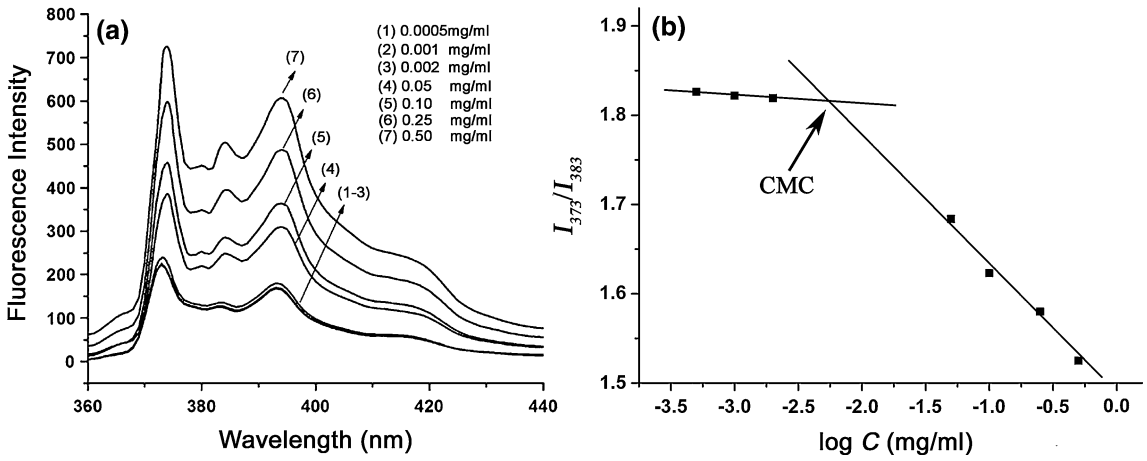

Fig. 2 **a** Fluorescence emission spectra of pyrene as a function of GA–PEG–PBLG concentration. **b** Plots of the intensity ratio (I_{373}/I_{383}) from pyrene excitation spectra versus log C of GA–PEG–PBLG

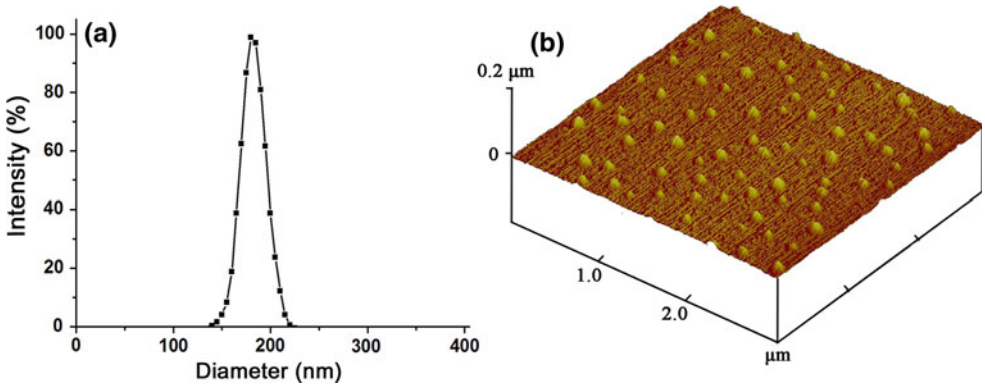

Fig. 3 **a** Size distribution histogram and **b** AFM image of GA–PEG–PBLG micelles

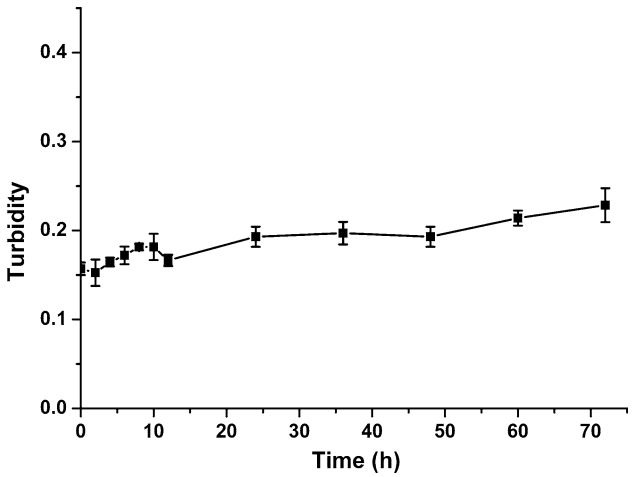

Fig. 4 Turbidity evaluation of GA–PEG–PBLG micelles in PBS containing 1 wt% BSA, mean ± SD ($n = 3$)

3.4 Drug encapsulation and in vitro release

To investigate the feasibility of GA–PEG–PBLG micelles as a liver-targeted drug carrier, anticancer drug DOX was incorporated into GA–PEG–PBLG micelles via diafiltration. DLC, DLE and diameters data are summarized in Table 1. A lower DOX/copolymer weight ratio resulted in higher DLE because of less DOX precipitation during encapsulation, which induced lower DLC. Besides, a lower DOX feed weight ratio also led to a smaller particle size. Similar results were found by Jeong for adriamycin-loaded polymeric micelles [38]. In comprehensive consideration of the particle size, DLC and DLE values, the optimal initial weight ratio of DOX to the copolymer was 0.1, which yielded a particle diameter of 214.2 nm, 7.5% DLC and 66.3% DLE. Unless otherwise specified, this ratio was used throughout the study.

It is of primary importance to reveal the release behavior of anticancer drugs from micelles as it may provide a foundation for minimizing systemic leakage of the drugs before it reaches the target site. Results in Fig. 5 show that the DOX release profiles is obviously affected by the pH. At pH 7.4, after initial release of approximately 20 wt% in the first day, DOX release reached a plateau in the following 6 days. However, at pH 5.8, the release was accelerated and over 45 wt% of DOX was released in the first day, followed by a constant slow release that approached 60 wt% in the next 6 days.

3.5 DOX biodistribution profiles

Animal studies were carried out to investigate the biodistribution of DOX·HCl and DOX/GA–PEG–PBLG micelles for 2 h after intravenous injection. Figure 6 exhibits the DOX levels in each tissue determined by spectrofluorometry. DOX·HCl had a wide distribution in tissues and was mainly concentrated in the lung (26.82 μg DOX/g lung), kidney (20.06 μg DOX/g kidney) and heart (14.5 μg DOX/g heart). However, the micelle formulation obviously accumulated in the liver (43.78 μg DOX/g liver), resulting in a 4.9-fold higher DOX concentration than that for the DOX·HCl group ($^{**}P < 0.01$).

3.6 MTT cytotoxicity assay

In vitro cytotoxicity against QGY-7703 cells was evaluated via MTT assay. No obvious cytotoxicity was detected for blank GA–PEG–PBLG micelles, even at a high micelle concentration (1 mg/ml) (data not shown). The cytotoxicities of DOX·HCl and DOX/GA–PEG–PBLG micelles are shown in Fig. 7. Cytotoxicity increased with the increasing DOX concentration, and the IC_{50} (50% inhibitory concentration) for DOX·HCl and DOX/GA–PEG–PBLG micelles was 90 and 47 ng/ml, respectively. Considering that only a small proportion of DOX was released from the micelles during incubation (Fig. 5), the actual cytotoxicity of DOX/GA–PEG–PBLG micelles would be more prominent.

The cytotoxicity of DOX/GA–PEG–PBLG micelles as a function of time and dosage was investigated against QGY-7703 cells and the results are summarized in Fig. 8. After 1 day of incubation, no appreciable cytotoxicity was

Table 1 Characterization of DOX/GA–PEG–PBLG micelles

Feed weight ratio (drug/copolymer)	DLC (%)	DLE (%)	Diameter (nm)
0	–	–	181.8
0.05	4.1	73.2	194.6
0.10	7.5	66.3	214.2
0.15	9.1	52.1	235.6
0.20	10.3	46.8	269.1

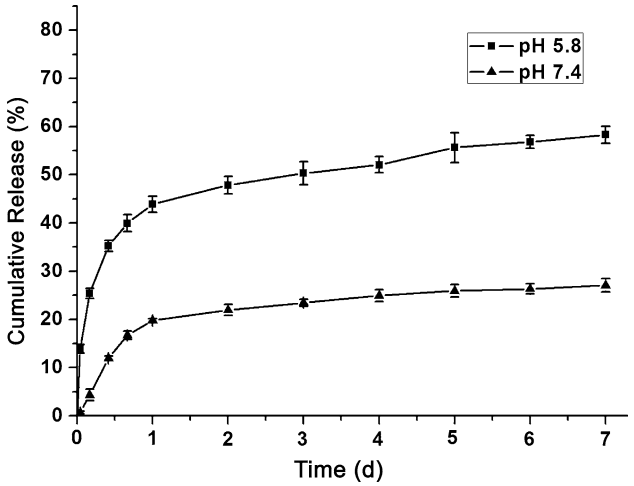

Fig. 5 In vitro DOX release behavior of DOX/GA–PEG–PBLG micelles under neutral (pH 7.4) and acid (pH 5.8) conditions, mean ± SD ($n = 3$)

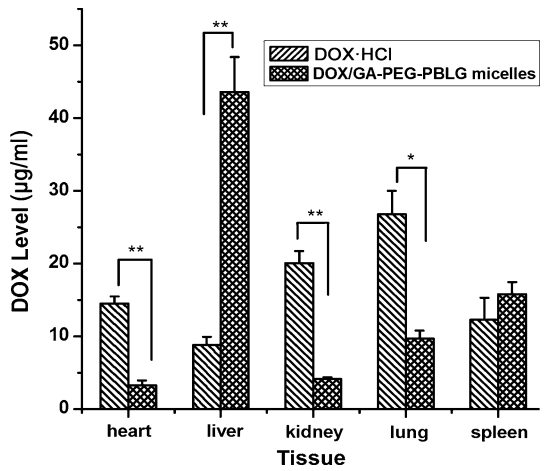

Fig. 6 Biodistribution profiles of DOX·HCl and DOX/GA–PEG–PBLG micelles in rats at 2 h after intravenous injection. Data presented as mean ± SD, $n = 5$. $^{*}P < 0.05$, $^{**}P < 0.01$ versus DOX·HCl group

detected for an effective DOX concentration lower than 0.20 μg/ml. By contrast, the rate of cell death drastically increased after 4 days of treatment with the same DOX concentration, indicating that sufficient DOX internalization within cells was achieved during this relatively long

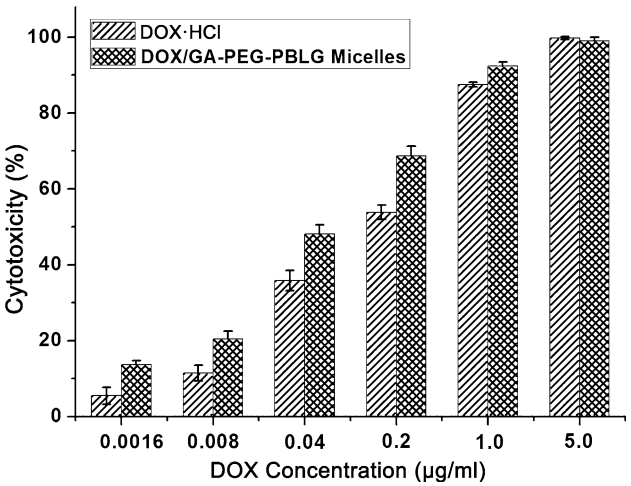

Fig. 7 In vitro cytotoxicity against QGY-7703 cells after the treatment with DOX·HCl or DOX/GA–PEG–PBLG micelles for 72 h, mean ± SD ($n = 3$)

incubation time. The IC_{50} was 1.11 and 0.07 μg/ml for incubation of 1 and 4 days respectively, which suggested that the effect was time-dependent. Moreover, after incubation for 1 day, only less than 20% of cell proliferation was suppressed at an effective DOX concentration below 0.20 μg/ml. However, almost 80% of cells were killed when the effective DOX concentration increased to 5.00 μg/ml, indicating a dosage-dependent effect.

4 Discussion

Liver cancer is one of the most prevalent cancers worldwide and the morbidity has increased year by year. Traditional pharmacotherapy is limited by the toxic side effects of the anticancer drugs used. Therefore, the

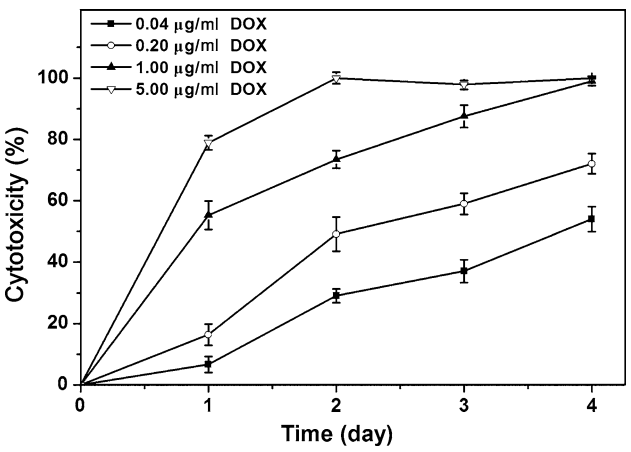

Fig. 8 Time- and dosage-dependent cytotoxicity of DOX/GA–PEG–PBLG micelles against QGY-7703 cells, mean ± SD ($n = 3$) (the *label* represents the effective DOX concentration in the micelles)

construction and development of new therapeutic strategies to treat liver cancer is very important. Liver targeting drug delivery system (LTDDS), that can ferry drugs to the desired site, is a highly desirable strategy to improve the therapeutic efficacy and reduce systematic side effects of drugs. And a number of scholars have studied liver-targeted drug delivery [6, 16, 39, 40].

At present, most studies have relied on the conjugation of carriers with liver targeting ligands, such as antibodies [6], galactose compounds [16, 40], to encapsulate drugs for targeted drug delivery to the liver. It is well known that the targeted effect of monoclonal antibodies is very effective [6]. However, most antibodies used in the system are derived from mice, the bio-security and bio-compatibility became a major concern. It had also been reported that asialoglycoprotein receptors (ASGPR), which is the specific receptor of ligands like galactose compounds, are over-expressed on the surface of hepatocytes. And ASGPR has been widely exploited for liver targeting [16, 40]. However, further studies demonstrated that there were inhibitors in serum of hepatopath which resulted in a low recognition extent of ASGRP for galactose residues [41]. Hence, the discovery of a new liver targeting ligand instead of the conventional one is primarily important.

Recently, GA has been proved to be enriched in liver. Thus, several groups have utilized GA as liver targeting ligand to modify drug carriers, which produced some interesting results [25, 26]. However, most current researches on the targeted property of GA still stay at the cellular level. There are few reports about GA as the targeted group in vivo. In our previous works, the liver targeting ability of GA-modified blank nanoparticles had been confirmed in vivo [23, 24]. In this study, the drug distribution of DOX-loaded micelles has been investigated in detail. Besides, the study about the cytotoxic effect of GA-modified particles on human liver cells is also particularly important, as it may provide a better and more practical understanding of the therapeutic efficacy of GA-mediated LTDDS.

4.1 Characterization of GA–PEG–PBLG copolymer

Poly(γ-benzyl L-glutamate), a synthetic polypeptide, has attracted intensive attention for biomedical applications because of its capacity to be both biocompatible as well as biodegradable to naturally-occurring biological products [42]. Besides, the carboxylic acid function in the side chain can be easily available after hydrolysis of the lateral benzyl ester, which could be further modified with multiple ligands. In this study, we focused our interest on the synthesis of PBLG derivatives using initiators allowing the preparation of biocompatible micelles possessing liver targeting ability.

The structure of GA–PEG–PBLG copolymer was confirmed by FT-IR and ^{1}H-NMR measurement, and the molecular weight of the copolymer was also verified by GPC. All the results showed that the copolymer was synthesized successfully.

4.2 Degradation behavior of GA–PEG–PBLG copolymer

Since the biodegradation of biomaterials is important for the use, so the degradation profile of the GA–PEG–PBLG copolymer was also studied in vitro. The fast degradation behavior in acidic conditions may be ascribed to the more reactivity of carbon from the carbonyl towards water, which was induced by the reaction of proton and oxygen of the carbonyl. It should be noted that although the hydrophilic PEG segment is non-degradable, it becomes water-soluble after extensive degradation of the GA–PEG–PBLG copolymer. Besides, PEG with a molecular weight less than 6×10^3 Da can be easily excreted by the kidney [43]. Although the in vitro degradation study was only carried out over 7 weeks, the trend in Fig. 1 demonstrates that GA–PEG–PBLG copolymer significantly degrades over time.

4.3 Stability of GA–PEG–PBLG micelles

A remarkably low CMC for micelles is crucial because this effectively prevents micelle dissociation on extreme dilution after intravenous injection into the body, thus allowing retention of the loaded drugs for a prolonged time before reaching the target site [44]. The emission spectra of pyrene in various concentrations of GA–PEG–PBLG copolymer were measured to investigate the micellar behavior of the copolymer in aqueous solution. Pyrene was chosen as the fluorescence probe because it can preferentially partition into hydrophobic microdomains with a change in molecular photophysical properties [45]. The results showed that the CMC value of GA–PEG–PBLG copolymer was only 7.16 μg/ml, which could insure the stability of nanoparticles in vivo.

In addition, once hydrophobic particles (such as PBLG and PLA) are administered in the body, they promptly suffer from opsonization due to enhanced adsorption of blood serum proteins on their surface, resulting in rapid recognition by the RES organs such as the liver and spleen. This phenomenon can be dramatically retarded by modifying the particle surface with a hydrophilic PEG chain [36]. As discussed above, the introduction of PEG endowed the GA–PEG–PBLG copolymer with an amphiphilic nature, which facilitated the formation of polymeric micelles with remarkably low CMC in aqueous solution. The hydrophilic PEG shell was exposed on the surface of the particles, which effectively generated steric repulsion and inhibited the undesirable adsorption of plasma proteins.

4.4 DOX encapsulation and release in vitro

The PBLG segment in the copolymer exhibits an α-helical conformation, which is hydrophobic and rigid enough to provide a favorable non-polar environment for the entrapment of hydrophobic DOX. Furthermore, π–π interaction between the benzyl moiety of the PBLG core and the aromatic ring of entrapped DOX may also contribute to retard drug release during transmission in vivo [44].

In Sect. 4.2, we discussed the in vitro degradation behavior of GA-PEG-PBLG copolymer under both pH conditions. Results showed that no weight loss was detected in the first week, indicating that the influence of pH on the micelles alone could be ignored in the drug release study. Thus, we inferred that the pH-dependent release behavior of DOX was probably due to reprotonation of the $-NH_2$ group in the sugar moiety of DOX, which resulted in a diminished hydrophobic interaction between the aromatic ring of DOX and the benzyl moiety of the PBLG segment [44, 46]. It is noteworthy that the pH-dependent release behavior is very important because it can maintain the micelles stable for a prolonged time under normal physiological conditions, which reduces undesirable side effects and heart cytotoxicity caused by DOX leakage. By contrast, faster release will occur once the micelles are internalized within tumor cells (pH $\sim$ 5.8) via endocytosis.

The drug release mechanism of the micelles was assessed under different pH conditions. Data were fitted using the Ritger–Peppas equation. As shown in Table 2, R^2 was above 0.9 in both cases, suggesting a good correlation for this model. Moreover, n values were all lower than 0.45, indicating that the release was mainly driven by a Fickian diffusion mechanism [34, 47]. In the release system, the initial burst drug in the targeted site could kill cancer cells effectively. Then the sustained release drugs could further suppress cell proliferation for a prolonged time. Certainly, we are aware that the in vivo drug release kinetics is much more complex than the theoretical one, which still needs abundant experiment for a further research.

4.5 DOX biodistribution in vivo

As previously reported, there are abundant GA receptors on the cellular membrane of rat liver. Therefore, improved cellular uptake of DOX/GA–PEG–PBLG micelles was achieved via GA-receptor-mediated endocytosis. Kupffer cells in rat liver may also account for the high accumulation of DOX in this organ. Since the spleen has similar physiological properties to the liver, it can also accumulate DOX at a level up to approximately 17 μg DOX/g spleen.

Notably, the DOX concentration in rat heart for the DOX/GA–PEG–PBLG micelle group was merely 3 μg DOX/g heart, which is much lower than that for the DOX·HCl group

Table 2 Drug release kinetic data for DOX/GA–PEG–PBLG micelles

pH of release media	Ritger–Peppas model			Transport mechanism
	(n)	(k)	(R^2)	
5.8	0.21	20.33	0.98	Diffusion controlled
7.4	0.32	5.69	0.93	Diffusion controlled

n Diffusion exponent, k kinetic constant, R^2 correlation coefficient

(**$P < 0.01$). The significantly lower DOX level in heart indicates that the cardiac toxicity of DOX was substantially reduced by incorporation within micelles. This result is encouraging since cardiac toxicity is a major side effect of DOX chemotherapy, limiting its full therapeutic exploitation in the clinic. In addition, lower DOX levels were also detected in kidney after incorporation in micelles, indicating that the glomerular filtration of DOX·HCl was effectively decreased. The significant change in the in vivo fate of a drug after incorporation within a macromolecular carrier has also been reported by Kopečková and co-workers [48].

4.6 Cytotoxicity to hepatic carcinoma QGY-7703 cells

The distinct cytotoxic effects can be ascribed to the different cellular uptake approaches for different DOX formulations. DOX is a DNA-damaging anthracycline agent that only exerts its cytotoxicity in cell nuclei [49]. However, cellular internalization approach for DOX·HCl is a passive diffusion manner, which suffers from rapid excretion from cells by P-glycoprotein (P-gp) pump effect [50], resulting in inadequate DOX concentrations within cells and further inducing a limited cytotoxic effect. In contrast, for DOX within micelles, a large amount of DOX could be delivered intracellularly in the form of nano-sized micelles via the endocytic pathway, which is more effective than a diffusion manner. Similar results were reported by Gao and co-workers for MCF-7 cells incubated with PEG-*b*-PCL micelles [46], and by Park and co-workers for KB-cells incubated with folate-modified polymeric micelles [51].

All of the above results significantly demonstrated that the incorporated DOX could still maintain its bioactivity effectively, which is primarily important for pharmaceutical applications.

5 Conclusions

We described the synthesis and characterization of GA-functionalized biodegradable poly(ethylene glycol)-*b*-poly-(γ-benzyl L-glutamate) (GA–PEG–PBLG) micelles for liver-targeted delivery of DOX. The in vitro drug release study revealed a pH-dependent release profile, with release

dominated by Fickian diffusion mechanism. The in vivo DOX distribution profile showed that micelles were particularly accumulated in rat liver, thus significantly decreasing the toxic side effects of anticancer drugs on non-target tissues. The DOX concentration in rat liver after micelles delivery was approximately 4.9-fold higher compared with DOX·HCl. DOX/GA–PEG–PBLG micelles exhibited almost twofold more potent cytotoxicity than DOX·HCl, and the cytotoxicity was time- and dosage-dependent. These preliminary results indicated that further study of GA-functionalized micelles as potential drug carriers for liver-specific targeting is warranted.

Acknowledgments The authors gratefully acknowledge the National Natural Science Foundation of China (No. 50873048, No.51073080) and Key Project of Scientific and Technical Supporting Programs of Tianjin (No. 10ZCKFSY07500) for the financial support. The authors also appreciate Prof. Hua Tang and Mr. Min Liu for their assistance in the cytotoxicity assay.

References

1. Ringsdorf H. Structure and properties of pharmacologically active polymers. J Polym Sci Polym Symp. 1975;51:135–53.
2. Soussan E, Cassel S, Blanzat M, et al. Drug delivery by soft matter: matrix and vesicular carriers. Angew Chem Int Ed. 2009;48:274–88.
3. Rapoport N. Physical stimuli-responsive polymeric micelles for anti-cancer drug delivery. Prog Polym Sci. 2007;32:962–90.
4. Meng FH, Zhong ZY, Jan FJ. Stimuli-responsive polymersomes for programmed drug delivery. Biomacromolecules. 2009;10: 197–209.
5. Nie Y, Zhang ZR, Li L, et al. Synthesis, characterization and transfection of a novel folate-targeted multipolymeric nanoparticles for gene delivery. J Mater Sci Mater Med. 2009;20:1849–57.
6. Chen ZN, Mi L, Xu J, et al. Targeting radioimmunotherapy of hepatocellular carcinoma with iodine (I-131) metuximab injection: clinical phase I/II trials. Int J Radiat Oncol. 2006;65:435–44.
7. Petrak K. Essential properties of drug-targeting delivery systems. Drug Discov Today. 2005;10:1667–73.
8. Lavasanifar A, Samuel J, Kwon GS. Poly(ethylene oxide)-*block*-poly(L-amino acid) micelles for drug delivery. Adv Drug Deliv Rev. 2002;54:169–90.
9. Allen C, Maysinger D, Eisenberg A. Nano-engineering block copolymer aggregates for drug delivery. Colloids Surf B Biointerfaces. 1999;16:3–27.
10. Kakizawa Y, Kataoka K. Block copolymer micelles for delivery of gene and related compounds. Adv Drug Deliv Rev. 2002;54: 203–22.
11. Harada A, Kataoka K. Supramolecular assemblies of block copolymers in aqueous media as nanocontainers relevant to biological applications. Prog Polym Sci. 2006;31:949–82.
12. Haag R. Supermolecular drug-delivery systems based on polymeric core-shell architectures. Angew Chem Int Ed. 2004;43: 278–82.
13. Allen TM. Ligand-targeted therapeutics in anticancer therapy. Nat Rev Cancer. 2002;2:750–63.
14. Sutton D, Nasongkla N, Blanco E, et al. Functionalized micellar systems for cancer targeted drug delivery. Pharm Res. 2007;24: 1029–46.
15. Morell AG, Irvine RA, Sternlieb I, Scheinberg IH. Physical and chemical studies on ceruloplasmin. Metabolic studies on sialic acid-free ceruloplasmin in vivo. J Biol Chem. 1968;243:155–9.
16. Liang HF, Chen CT, Chen SC, et al. Paclitaxel-loaded poly(γ-glutamic acid)-poly(lactide) nanoparticles as a targeted drug delivery system for the treatment of liver cancer. Biomaterials. 2006;27:2051–9.
17. Zhang J, Zhang QS, Chen XM, et al. Synthesis of a targeting drug for antifibrosis of liver; a conjugate for delivering glycyrrhetin to hepatic stellate cells. Glycoconj J. 2003;19:423–9.
18. Zhang YL, Wu Y, Yang WL, et al. Preparation, characterization, and drug release in vitro of chitosan-glycyrrhetic acid nanoparticles. J Pharm Sci. 2006;95:181–91.
19. Negishi M, Irie A, Nagata N, et al. Specific binding of glycyrrhetinic acid to the rat liver membrane. Biochim Biophys Acta. 1991;1066:77–82.
20. Ismair MG, Stanca C, Ha HR, et al. Interactions of glycyrrhizin with organic anion transporting polypeptides of rat and human liver. Hepatol Res. 2003;26:343–7.
21. Zha RT, He XT, Du T, et al. Synthesis and Characterization of chitosan nanoparticles modified by glycyrrhetinic acid as a liver targeting drug carrier. Chem J Chin U. 2007;28:1098–100.
22. Tsuji H, Osaka S, Kiwada H. Targeting of liposomes surface-modified with glycyrrhizin to the liver. I. Preparation and biological disposition. Chem Pharm Bull. 1991;39:1004–8.
23. Tian Q, Wang XH, Wang W, et al. Insight into glycyrrhetinic acid: the role of the hydroxyl group on liver targeting. Int J Pharm. 2010;400:153–7.
24. Tian Q, Zhang CN, Wang XH, et al. Glycyrrhetinic acid-modified chitosan/poly(ethylene glycol) nanoparticles for liver-targeted delivery. Biomaterials. 2010;31:4748–56.
25. Lin AH, Liu YM, Huang Y, et al. Glycyrrhizin surface-modified chitosan nanoparticles for hepatocyte-targeted delivery. Int J Pharm. 2008;359:247–53.
26. Mao SJ, Bi YQ, Jin H, et al. Preparation, characterization and uptake by primary cultured rat hepatocytes of liposomes surface-modified with glycyrrhetinic acid. Pharmazie. 2007;62:614–9.
27. Cha RT, Du T, Li JH, et al. Synthesis and characterization of polypeptide containing liver-targeting group. Polym Int. 2006;55: 1057–62.
28. Daly WH, Phche D. The preparation of N-carboxyanhydrides of α-amino acids using *bis*(trichloromethyl) carbonate. Tetrahedron Lett. 1998;29:5859–62.
29. Van-Steenis JH, van Maarseveen EM, Verbaan FJ, et al. Preparation and characterization of folate-targeted pEG-coated pDMA-EMA-based polymers. J Control Release. 2003;87:167–76.
30. Barbosa MEM, Montembault V, Cammas-Marion S, et al. Synthesis and characterization of novel poly(γ-benzyl-L-glutamate) derivatives tailored for the preparation of nanoparticles of pharmaceutical interest. Polym Int. 2007;56:317–24.
31. Vey E, Roger C, Meehan L, et al. Degradation mechanism of poly(lactic-co-glycolic) acid block copolymer cast films in phosphate buffer solution. Polym Degrad Stab. 2008;93:1869–76.
32. Jeong YI, Nah JW, Lee HC, et al. Adriamycin release from flower-type polymeric micelle based on star-block copolymer composed of poly(γ-benzyl L-glutamate) as the hydrophobic part and poly(ethylene oxide) as the hydrophilic part. Int J Pharm. 1999;188:49–58.
33. Huang CK, Lo CL, Chen HH, et al. Multifunctional micelles for cancer cell targeting, distribution imaging, and anticancer drug delivery. Adv Funct Mater. 2007;17:2291–7.
34. Peppas NA. A model of dissolution-controlled solute release from porous drug delivery polymeric systems. J Biomed Mater Res. 1983;17:1079–87.
35. Kim D, Gao ZG, Lee ES, et al. In vivo evaluation of doxorubicin-loaded polymeric micelles targeting folate receptors and early

endosomal pH in drug-resistant ovarian cancer. Mol Pharm. 2009;6:1353–62.
36. Segura-Sánchez F, Montembault V, Fontaine L, et al. Synthesis and characterization of functionalized poly(γ-benzyl-L-glutamate) derivates and corresponding nanoparticles preparation and characterization. Int J Pharm. 2010;387:244–52.
37. Martinez-Barbosa ME, Cammas-Marion S, Bouteiller L, et al. PEGylated degradable composite nanoparticles based on mixtures of PEG-*b*-Poly(γ-benzyl L-glutamate) and poly(γ-benzyl L-glutamate). Bioconjug Chem. 2009;20:1490–6.
38. Jeong YI, Na HS, Cho KO, et al. Antitumor activity of adriamycin-incorporated polymeric micelles of poly(γ-benzyl L-glutamate)/poly(ethylene oxide). Int J Pharm. 2009;365:150–6.
39. He Q, Yuan WM, Liu J, et al. Study on in vivo distribution of liver-targeting nanoparticles encapsulating thymidine kinase gene (TK gene) in mice. J Mater Sci Mater Med. 2008;19:559–65.
40. Wu DQ, Lu B, Chang C, et al. Galactosylated fluorescent labeled micelles as a liver targeting drug carrier. Biomaterials. 2009;30:1363–71.
41. Stockert RJ, Morell AG. Hepatic binding protein: the galactose-sepcific receptor of mammalian hepatocytes. Hepatology. 1983;3:750–7.
42. Upadhyay KK, Bhatt AN, Mishra AK, et al. The intracellular drug delivery and anti tumor activity of doxorubicin loaded poly(γ-benzyl L-glutamate)-*b*-hyaluronan polymersomes. Biomaterials. 2010;31:2882–92.
43. Zweers MLT, Engbers GHM, Grijpma DW, et al. In vitro degradation of nanoparticles prepared from polymers based on DL-lactide, glycolide and poly(ethylene oxide). J Control Release. 2004;100:347–56.
44. Kataoka K, Matsumoto T, Yokoyama M, et al. Doxorubicin-loaded poly(ethylene glycol)-poly (β-benzyl-L-aspartate) copolymer micelles: their pharmaceutical characteristics and biological significance. J Control Release. 2000;64:143–53.
45. Li YY, Zhang XZ, Cheng H, et al. Novel stimuli-responsive micelle self-assembled from Y-shaped P(UA-Y-NIPAAm) copolymer for drug delivery. Biomacromolecules. 2006;7:2956–60.
46. Shuai XT, Ai H, Nasongkla N, et al. Micellar carriers based on block copolymers of poly(ε- caprolactone) and poly(ethylene glycol) for doxorubicin delivery. J Control Release. 2004;98:415–26.
47. Siepmann J, Siepmann F. Mathematical modeling of drug delivery. Int J Pharm. 2008;364:328–43.
48. Shiah JG, Dvořák M, Kopečková P, et al. Biodistribution and antitumour efficacy of long- circulating N-(2-hydroxypropyl) methacrylamide copolymer-doxorubicin conjugates in nude mice. Eur J Cancer. 2001;37:131–9.
49. Zunino F, Marco AD, Zaccara A, Gambetta RA. The interaction of daunorubicin and doxorubicin with DNA and chromatin. Biochim Biophys Acta. 1980;607:206–14.
50. Itsubo M, Ishikawa T, Toda G, et al. Immunohistochemical study of expression and cellular localization of the multidrug resistance gene product P-glycoprotein in primary liver carcinoma. Cancer. 1994;72:298–303.
51. Yoo HS, Park TG. Folate receptor targeted biodegradable polymeric doxorubicin micelles. J Control Release. 2004;96:273–83.